NUMERICAL ANALYSIS OF SPECIES DIFFUSION AND METHANOL DECOMPOSITION IN THERMOCATALYTIC REACTOR BASED ON THE INTERMETALLIC PHASE OF Ni_3Al FOR LOW REYNOLDS NUMBERS

PAWEŁ ZIÓŁKOWSKI[1,4], MICHAŁ STAJNKE[1], PAWEŁ JÓŹWIK[2], ZBIGNIEW BOJAR[2], PIOTR JÓZEF ZIÓŁKOWSKI[1,3*] AND JANUSZ BADUR[1**]

[1] *Energy Conversion Department*
The Szewalski Institute of Fluid-Flow Machinery PAS-ci
Fiszera 14, 80-231 Gdańsk, Poland

[2] *Faculty of Advanced Technologies and Chemistry*
Military University of Technology
Gen. Witolda Urbanowicza 2, 00-908 Warsaw 46, Poland

[3] *Faculty of Civil and Environmental Engineering*
Gdańsk University of Technology
Narutowicza 11/12, 80-233 Gdańsk, Poland

[4] *Faculty of Mechanical Engineering, Gdańsk University of Technology*
Narutowicza 11/12, 80-233 Gdańsk, Poland

*Corresponding authors: *pziolkowski@imp.gda.pl, **jb@imp.gda.pl*

(received: 10 April 2018; revised: 16 May 2018;
accepted: 25 June 2018; published online: 8 July 2018)

Abstract: Numerical modelling of hydrogen production by means of methanol decomposition in a thermocatalytic reactor using corrugated foil made of the Ni_3Al intermetallic phase is shown in the paper. Experimental results of the flow analysis of mixtures containing helium and methanol in a thermocatalytic reactor with microchannels were used for the initial calibration of the CFD calculations (calculations based on the Computational Fluid Dynamics method). The reaction of the thermocatalytic methanol decomposition was modelled based on experimental data, considering the size of the active surface. The drop in the methanol concentration at

the inlet to the reactor, ten millimetres in front of the thermocatalytic region, is associated with the diffusion of streams of other components, mainly hydrogen and carbon monoxide. The commercial CFD code was expanded by User Defined Functions (UDFs) to include surface chemical reaction rates in the interphase between the fluid and the solid. Extrapolation of data by means of the implemented numerical model enabled the assessment of the minimum length of microreactor channels and prediction of the optimal dimension at the system outlet. The results obtained by means of numerical calculations were calibrated and compared with the experimental data, confirming a satisfactory consistency of the data.

Keywords: CFD, thermocatalytic reactor, intermetallic phase of Ni_3Al

DOI: https://doi.org/10.17466/tq2018/22.3/b

1. Introduction

Ni-based catalysts exhibit an extremely high catalytic activity in methanol decomposition and synthesis of other gasses and promote production of carbon nanostructures (mainly carbon nanotubes) [1, 2]. One of the Ni-based, solid-state catalysts is the Ni_3Al intermetallic phase and its alloys [3], which belongs to a sort of multifunctional materials, combining properties of both the structural and functional materials. According to the literature, Ni_3Al intermetallic thin foils exhibit extremely high catalytic properties in hydrocarbon decomposition reactions [4]. On the other hand, also based on the literature, the main disadvantage of this material is the relatively high temperature of the maximal hydrocarbon conversion [1, 5]. Nevertheless, the high temperature of the process can be utilized by placing a regenerative heat exchanger downstream of the reactor [3]. Therefore, the thermocatalytic reactor with thin strips or thin foils based on the Ni_3Al intermetallic phase produced according to the technology presented by Jóźwik *et al.* in the works [1, 3] appears as an innovative and extremely promising technology in the making. One example of an alloy foil package based on the intermetallic phase Ni_3Al, constructed as a rolled up honeycomb structure, is shown in Figure 1 (a). The micro-reactor generally consists of microchannels which are separated by a thin solid wall, as is highlighted schematically in Figure 1 (b). The cross section of the micro-channels with the characteristic dimensions in a honeycomb set is presented in Figure 1 (c).

1.1. Motivation

The appropriate selection of the device dimensions in such a way that the contact time of the flow across the catalytically active surface of the substrate providing the reaction of the target product is very important. In addition to experimental studies, work focused on the modeling of the thermocatalytic processes is becoming increasingly interesting. In addition to these works that describe in general the processes of chemical reactions [6–8] there are articles concerning models of reactors and catalytic micro-reactors [9, 10].

This paper is a continuation of the analysis of the presented geometry of a single microchannel [9]. However, different issues have been considered, namely the catalytic surface reactions of the decomposition of methanol and the volume reaction of shifting or methanation inside a microchannel. Generally, it is

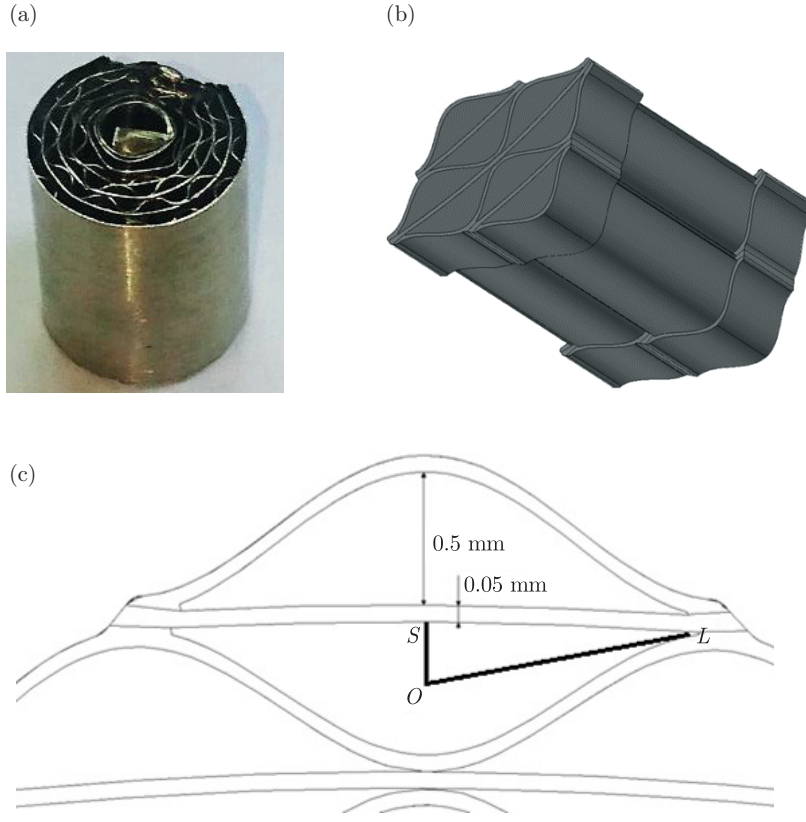

Figure 1. (a) Example of microreactor core – packaging of smooth and corrugated Ni_3Al foils wound in a honeycomb structure; (b) eight individual microchannels starting from the inlet to the packet and ending at the outlet of the packet, accepted for numerical simulation; (c) the characteristic dimensions of the reactor

widely known that the catalytic surface reactions, in the direct vicinity of walls coated with active layers, are very often present in technical situations [11, 12]. For thermal decomposition reactions, these active layers are often built on the base of Ni alloys [2, 13, 14]. As previously mentioned in this paper, one of the most promising potential applications of the thin alloy foils, based on the intermetallic phase Ni_3Al with a high thermocatalytic activity, is within the field of air purification and removal of harmful substances and the controlled decomposition of hydrocarbons, and extended consideration is given here. In this study, the thermocatalytic reactor with microchannels was numerically considered with respect to the production of hydrogen. The main focus of this paper is to describe the mathematical modeling of the chemical surface reactions of the flow of a helium and methanol mixture. The model was verified and the performance of the thermocatalytic reactor with microchannels within the hydrogen production regime was investigated.

2. Numerical model

A mathematical model of the thermocatalytic micro-reactor is based on the elementary balance equations solved for fluids to include continuity, momentum, energy, evolution of kinetic energy of turbulence, evolution of dissipation of kinetic energy of turbulence and species transport within the frame of the finite volume method (FVM). The governing equations for the whole device model can be given in the following compact with the CFD form:

$$\frac{\partial}{\partial t}\begin{Bmatrix}\rho\\ \rho\mathbf{v}\\ \rho e\\ \rho k\\ \rho\varepsilon\\ \rho Y_m\end{Bmatrix}+\operatorname{div}\begin{Bmatrix}\rho\mathbf{v}\\ \rho\mathbf{v}\otimes\mathbf{v}\\ \rho e\mathbf{v}\\ \rho k\mathbf{v}\\ \rho\varepsilon\mathbf{v}\\ \rho Y_m\mathbf{v}\end{Bmatrix}+\operatorname{div}\begin{Bmatrix}0\\ p\mathbf{I}\\ p\mathbf{v}\\ 0\\ 0\\ 0\end{Bmatrix}=\operatorname{div}\begin{Bmatrix}0\\ \mathbf{t}^t\\ \mathbf{t}^t\mathbf{v}+\mathbf{q}^t\\ \mathbf{J}_k\\ \mathbf{J}_\varepsilon\\ \mathbf{J}_m\end{Bmatrix}+\begin{Bmatrix}0\\ \rho\mathbf{S}_\mathbf{v}\\ \rho S_e\\ \rho S_k\\ \rho S_\varepsilon\\ \rho S_m\end{Bmatrix} \tag{1}$$

In the above, $\rho=\rho(\mathbf{x},t)$ is the mixture density that depends, in general, on the gas component m, time t and location $\mathbf{x}$, $\mathbf{v}=\mathbf{v}_i\mathbf{e}_i$ – the velocity vector, $\mathbf{e}_i$ – the versor in direction i, v_i – the vector value. Next, in the second row $\rho\mathbf{v}$, there are the bulk momentum density vectors, p is the thermodynamic pressure, $\mathbf{I}=\delta_{ij}\mathbf{e}_i\otimes\mathbf{e}_j$ defines the unit tensor, δ_{ij} is the Kronecker delta. $\mathbf{t}^t=\mathbf{t}^{\text{lam}}+\mathbf{t}^{\text{tur}}$ takes into account the total diffusive momentum flux (the flux components of the viscous stress, namely, laminar and turbulent, respectively), $\rho\mathbf{S}_\mathbf{v}$ includes all momentum sources. Additionally, the total specific energy $e=u+\frac{1}{2}\mathbf{v}^2$ is a sum of specific internal energy u and specific kinetic energy $\frac{1}{2}\mathbf{v}^2$, $\mathbf{q}^t$ represents the total diffusive heat flux, and S_e are the energy sources. Furthermore, in the evolution part of the kinetic energy of turbulence k and the dissipation of the kinetic energy of turbulence ε, there occur diffusive fluxes of k and a diffusive flux of ε, *i.e.* $\mathbf{J}_k$, $\mathbf{J}_\varepsilon$, respectively, and sources, namely, the source of the kinetic energy of turbulence S_k together with the source of the dissipation of the kinetic energy of turbulence S_ε. Finally, Y_m is the mass fraction of the gas component $m=$ He; CH_3OH; CO; H_2; CH_4; H_2O; CO_2, S_m are the creation/destruction sources of species m and $\mathbf{J}_m$ defines the flux of m components of the mixture. A more detailed description of Equation (1) is presented in [6].

2.1. Chemical reactions

The main products of the methanol decomposition reaction over the Ni_3Al foils are the hydrogen, carbon monoxide and solid carbon deposits. The by-products are carbon dioxide, methane and water [5, 13, 14]. In the simplest case, the methanol decomposition may be described by the following equation [14]:

$$CH_3OH\rightarrow CO+2H_2 \tag{2}$$

If we consider the thermocatalytic microreactor fed by methanol via the decomposition reaction, it should be noticed that carbon monoxide and hydrogen, which are the products, can be consumed in the reacting flow via the following methanation reaction:

$$CO + 3H_2 \rightarrow CH_4 + H_2O \tag{3}$$

The carbon monoxide component is converted into carbon dioxide via a shift reaction. We decided to employ a simplified single-step non-reversible reaction in the form of:

$$CO + H_2O \rightarrow CO_2 + H_2 \tag{4}$$

Carbon deposition can be considered through the Boudouard reaction:

$$2CO \rightarrow C + CO_2 \tag{5}$$

It should be mentioned that some of the by-products, especially water, can oxidize the Ni_3Al catalyst surface. Based on the paper [5], where H_2O is the by-product of methanol decomposition and can be used to create the metallic Ni and also can be converted into aluminum hydroxide. It is worth noting that the appearing Ni nanoparticles can be oxidized by H_2O according to the reaction, and it can then also take part in the subsequent reaction of the spinel formation.

2.2. Methanol decomposition source

As has been already mentioned, changes of the gas component, m, concentration in the mixture due to chemical reactions can be implemented via a volumetric or surface source term, S_m, in the species transport Equation (1). At this point it should be emphasized that numerous problems of the gas-dynamic boundary layer increase as a result of combination with the chemical phenomena that are taking place in the vicinity of solids. The flow model of chemical reactions, discussed in many works [6–8] refers to mechanical, thermal and chemical issues of the event occurring in the volume. The phenomena occurring on the surface of the thermocatalytic reactor (or the combustion chamber) are characterized by complete anisotropy. Apart from the volume production of the component, S_m, the reaction of the surface absorption also describes the chemical kinetics, and therefore they should be treated as some surface source (or discounts) for the gas component [15, 16].

It is assumed in the numerical case that there is no coke creation during the micro-reactor operation and the products of thermocatalytic oxidation are not deposited on the catalyst surface. Hence, to provide a complete CFD model of the catalytic micro-reactor, it will be necessary to consider the coke deposition phenomena. In the future, the wall boundary conditions (temperature and emissivity) should be corrected to account for the effects of this deposit accumulation under the conditions of this reaction. Examples of publications that consider ash deposition and temperature fields, may be found as [17–19], and could be helpful in the future works including the growth of carbon nanotubes. In this paper, it is also assumed that there are no site species involved in the surface reactions, and hence, it is only gas phase species that are modeled. For modeling purposes it is only the methanol decomposition reaction that is catalytic, so it is assumed that the source term, S_{CH_3OH}, can be formulated for methanol in finite volumes

strictly adjacent to the micro-reactor wall. The source of the decomposition of methanol (S_{CH_3OH}) depends on the catalytic properties of the intermetallic phase of Ni_3Al, and can be expressed via the following equation:

$$S_{CH_3OH} = W_{CH_3OH}\nu_{CH_3OH}\left(k_{Ni_3Al}[X_{CH_3OH}]\frac{A_{Ni_3Al}}{V_{cell}}\right) \tag{6}$$

where: $\nu_{CH_3OH(\alpha)}$ – the molar stoichiometric coefficient for CH_3OH and α^{th} non-reversible reaction and W_{CH_3OH} the molecular mass of methanol, kg/kmol. To obtain the volumetric source term, S_{CH_3OH}, the surface reaction rate should be divided by the height of the computational cell adjacent to the microreactor wall (A_{cat}/V_{cell}). It should be added that the source of methanol decomposition S_{CH_3OH} is then usually given as a function of the methanol molar concentration $\left[X_{CH_3OH}\right]$ and the forward catalytic rate constant k_{cat}. There exists no proper data for a full model validation. Partially, it can be done through the methanol conversion to the reaction time characteristics diagram that is often available for a particular thermocatalytic micro-reactor. The kinetic mechanism was simplified by introducing a one step reaction.

2.3. Diffusion of mixture components

For methanol and other component concentrations, it is necessary to consider the effect of diffusive fluxes, such as the ordinary molecular diffusion in gas channels as well as the Knudsen diffusion. As was presented in the work [10, 20], the Knudsen diffusion is neglected for the considered geometry of the thermocatalytic microreactor. In general, diffusion flux $\mathbf{J}_m$ depends on the diffusion velocity $\mathbf{V}_m$ in the following way:

$$\mathbf{J}_m = \rho Y_m \mathbf{V}_m \tag{7}$$

The best proven closure on $\mathbf{V}_m$ is Dixon-Lewis' formula [6]:

$$\mathbf{V}_m = \frac{1}{X_m \bar{W}} \sum_{m' \neq m}^{NS} W_{m'} D_{mm'} \nabla X_{m'} - \frac{D_m^T}{\rho Y_m}\frac{\nabla T}{T} \tag{8}$$

where: $D_{mm'}$ and D_m^T, are the coefficients of multi-components and temperature diffusion, respectively, $W_{m'}$ is the molecular mass of component $m' \neq m$, the average molecular mass of components, $\bar{W}$, while T is the temperature in the reactor.

3. Analysis

3.1. Experiment and constant to calibration

In the examinations the thin Ni_3Al foils with thickness of about 50 μm and the average grain size of γ' phase in the Ni_3Al structure equal to about 15 μ m were tested. The stability test for the Ni_3Al catalyst in the methanol decomposition to hydrogen was carried out in a flow reactor, under an atmospheric pressure, at 500°C. In this case, the Ni_3Al foil was heated in the reactor and

a vapor mixture containing 40% vol. of methanol was introduced into the reactor ($W/F = 1.5\,(\mathrm{g_{cat}s})/\mathrm{cm}^3$). The desired methanol concentration in the gas phase was obtained by bubbling helium through a methanol saturator held at 43°C. The reaction mixture was analyzed *on-line* on TCD-GC (HP 5890 Series II) equipped with a Porapak Q packed column. Helium was used as the carrier gas in GC. All the lines were heated above 100°C to prevent water and methanol from condensation. The thermocatalytic decomposition rate of methanol $q_{\mathrm{CH_3OH}}$ presented in Table 1 was employed for validation purposes. Other parameters were treated as the boundary conditions for CFD calculations.

Table 1. An experimental thermocatalytic decomposition rate of methanol $q_{\mathrm{CH_3OH}}$ over the Ni_3Al foil estimated at $\dot{Q}_{\mathrm{mix}} = 35.1\,\mathrm{cm}^3/\mathrm{min}$ under the lowest possible temperature of the catalysis process which is sufficient to obtain a full conversion from the initial mole fraction *i.e.* $X_{\mathrm{CH_3OH}} = 0.4$

Parameter	Unit	Value
Total mass of catalytic specimens	g	0.777
W/F (weight/flow)	$(\mathrm{g_{cat}s})/\mathrm{cm}^3$	1.48
Conversion of methanol	%	100
Experimental reaction rate of methanol	$\mathrm{g}/(\mathrm{g_{cat}s})$	1.39

3.2. Numerical boundary condition

The recalculation of the experimental reaction rate and the diffusion flux were performed under the following assumptions: 1) constant temperature of the process; 2) a monolithic structure of the reactor; 3) the conversion parameters as in Table 1; 4) the geometric dimensions as presented in Figure 1 (c). Therefore, the temperature diffusion part is neglected and it is only $D_{mm'}$ that is considered in a numerical way. The methanol and helium mixture composition employed in the present analysis (Table 2) was based on the actual experimental data from one of the considered cases.

Table 2. Mixture of the methanol and helium composition

Component	Mass fraction (—)
Helium He	0.158
Carbon C	0.316
Hydrogen H	0.105
Oxygen O	0.421
Total	1.000

Microchannels coupled at the inlet and outlet are shown in Figure 1 (b). The velocity was assumed at the level of $v = 1\,\mathrm{cm/s}$. It is also known that the lowest possible temperature of the catalysis process sufficient to obtain a complete conversion occurred at $T = 500$°C. For the steady state flow analysis a CFD

commercial solver, namely Fluent, was used. This finite volume based code permits solving the three-dimensional fluid and heat flow problems concerned with turbulent structures and chemical reactions [21–23]. However, it also allows the addition of user defined subroutines programmed in C++ for problems that fall outside the capability of a standard version of the code. As has been demonstrated in recent works [24–26], in modeling flows with a strong interaction of the surface and liquid material, the boundary conditions and an appropriate closure in mathematical models are essential.

The grid used in the numerical calculations presented here consist of 1 600 000 finite volumes. This enables the model to maintain a high accuracy of the results, without consuming any unnecessary computing power. The channels beginning at the inlet into the package and terminating at the outlet from the package were divided into some blocks that were discretized by means of a structured numerical grid, steeply refined in the normal wall direction. Initial tests allowed the numerical grid to be used to ensure that further refinement did not influence the computational results. In the microreactor, a k-ε a turbulent approach was applied due to necessity of utilizing the Eddy-Dissipation model which was considered as the simplest one to work through using UDF. Regarding the fact that Reynold's numbers were very small we assumed that the turbulence model did not affect the results in a significant way. Therefore, the k-ε model was chosen as the most widely applied one. It was also assumed that the surface structure of the micro-reactor could be treated as homogeneous.

The standard SIMPLE (semi-implicit method for pressure-linked equations) method was used for the pressure-velocity coupling. The second order upwind schemes were employed for the convection term solution in the governing equations. The diffusion terms were central-differenced with the second order accuracy as well.

4. Results and discussion

Thermocatalytic decomposition of methanol in a single package micro-reactor is considered as a complicated phenomenon where the main products of the reaction are hydrogen and CO (see Equation (2)). Considering the obtained experimental results, with respect for the start (TOS = 0 min) and the equilibrium state of process (TOS = 270 min), a high influence of the diffusion flux can be concluded (Figure 2).

The distribution of the components due to the impact of different processes can be managed by: 1) diffusion effects; 2) mixing effects due to the eddy turbulence; 3) thermocatalytic surface decomposition and 4) volumetric reactions. The hydrogen mole fraction distribution at the eight single microchannels with an inlet into the package and an outlet from the package is presented in Figure 3.

As is highlighted in Figure 3 three main areas can be distinguished for the whole package: firstly, the diffusion flux area before microchannels (between $L = -10$ mm and $L = 0$ mm); secondly, the thermocatalytic reaction area (between

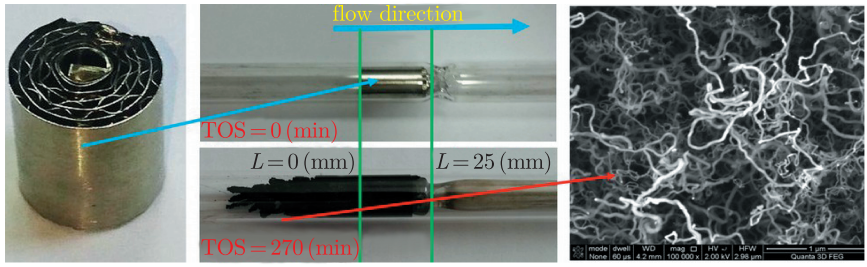

Figure 2. Honeycomb for start (TOS = 0 min) and equilibrium state of process (TOS = 270 min)

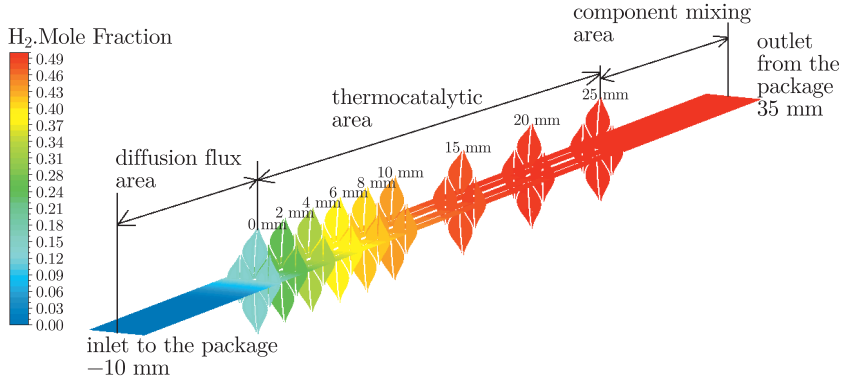

Figure 3. Hydrogen mole fraction X_{H_2} distribution at eight single microchannels beginning at package inlet and terminating at package outlet

$L = 0$ mm and $L = 25$ mm) and thirdly, the flow mixing area (between $L = 25$ mm and $L = 35$ mm). It is worth mentioning that the average Reynolds number in the domain is equal to 0.06 while the maximum value is around 0.2. The methanol mole fraction maximum is located at the beginning of the inlet package and decreases between the centre of the diffusive flux area and the thermocatalytic area in the microchannels, while further diminishing due to the surface catalytic reaction on the Ni_3Al thin foil, as presented in Figure 4. It should be understood that a decrease in the methanol concentration in the diffusion flux area is connected with diffusion fluxes of other components, mainly hydrogen and carbon monoxide (see Equations (1) and (7)). A change in the average mole fraction of hydrogen, methanol, carbon monoxide, steam, methane and carbon dioxide as a function of the reactor length L is shown in Figure 4.

A decrease in the CH_3OH concentration in the direction of the outlet from the package is related directly to the decomposition effects connected with the properties of the intermetallic phase of Ni_3Al, which is highlighted in Figure 4. The view of the local changes in the field of the hydrogen mole fraction in both the axial-sectional and the cross-sectional directions is illustrated in Figure 3, thus, the effects of the diffusion and the chemical reaction are clearly demonstrated.

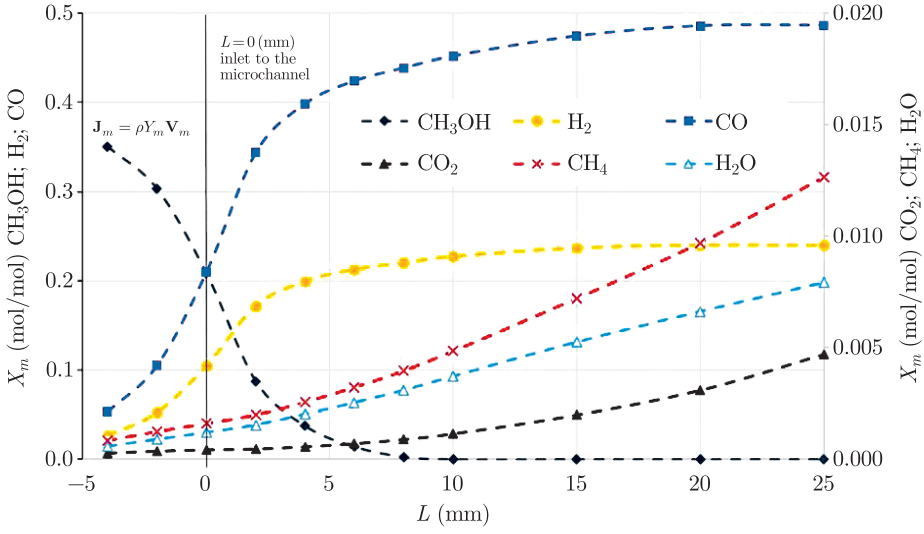

Figure 4. Change of averaged cross-sectional mole fraction X_m of hydrogen, methanol, carbon monoxide, steam, methane and carbon dioxide as function of reactor length L

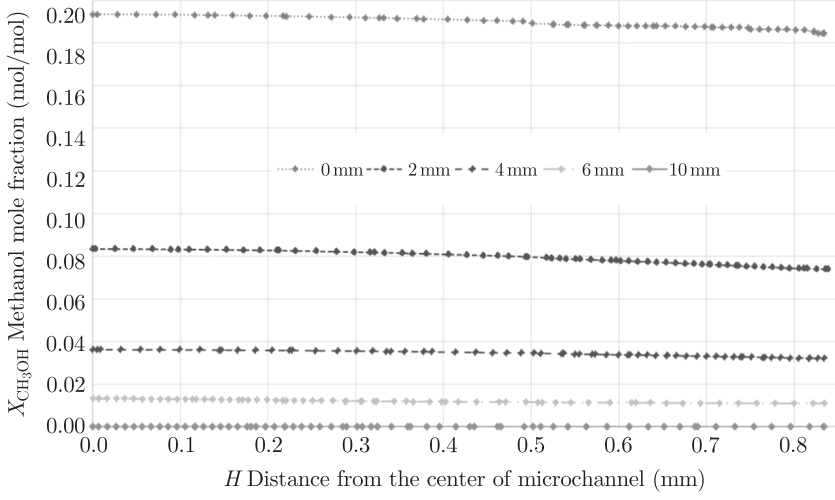

Figure 5. Change of local mole fraction of methanol in function of distance from the center of microchannel H, where of straight line length $|OL| = 0.834$ (mm) for consecutive cross sections $L = 0$; 2; 4; 6; 10 mm

The estimated average values in the cross section of the methanol mole concentrations have a visible tendency towards a changing rate of the decrease in the mole concentrations as a function of the reactor length L. Similar trends for a hydrogen and carbon monoxide increase are correlated with the surface reaction and a strong influence of the diffusion migration of the products of this reaction. Full thermocatalytic decomposition of methanol occurs at $L = 10$ mm into the microchannel from the inlet (Figure 4 and Figure 5), and from this point the

volumetric reactions of shifting and methanation reveal a tendency to outweigh the decomposition reactions, however, the mole fractions of $CH_4; H_2O; CO_2$ are about ten times lower than the mole fractions of H_2 or CO.

It should be mentioned that a change of the local mole fraction of methanol is a function of the distance as measured from the center of microchannel H, where the length of the $|OL|$ segment is equal to 0.834 (mm) for the consecutive cross sections $L = 0; 2; 4; 6; 10$ mm is presented in Figure 5. The $|OL|$ segment has been chosen to highlight the effect of contiguity of the catalytic surface especially in the corner of the microchannel at point L. The character of the change of the methanol mole fraction discloses that the influence of the diffusion is high not only in the axial direction (see Figure 4), but also on the surface perpendicular to the flow (see Figure 5). An obvious confirmation that the lowest concentration of methanol in the cross section is located directly on the surface interaction with Ni_3Al is pointed out in Figures 5–6. The methanol mole fraction across the $|OL|$ segment in different cross sections of the reactor retains a planar character so the local values X_m are approaching the average values in Figure 4.

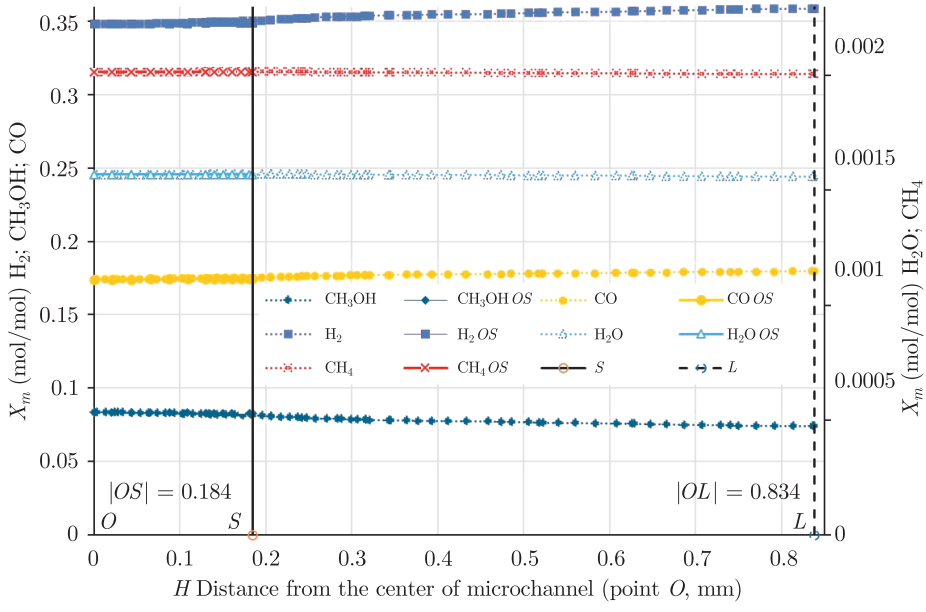

Figure 6. Change of local mole fraction X_m of hydrogen, methanol, carbon monoxide, steam and methane in function of distance from the centre of microchannel H (mm), where straight line length $|OL| = 0.834$ (mm) and $|OS| = 0.184$ (mm) for cross section $L = 2$ mm

Based on Figure 5 the cross section $L = 2$ mm has been selected to show the changes of the local mole fraction of components such as: hydrogen, methanol, carbon monoxide, steam and methane as a function of distance from the centre of microchannel H. It should be added that the distribution of each species from

the longest $|OL|$ segment has been compared to the distribution of each species from the shortest $|OS|$ segment (see Figure 6).

The visible changes of the local mole fraction X_m occur for components such as: hydrogen, methanol, carbon monoxide. In contrast, steam and methane as a function of distance from the centre of microchannel H (mm) are flat and almost parallel to each other, as presented in Figure 6. Therefore, the two characteristic dimensions of the thermocatalytic reactor, the length of the shortest segment in the cross section of the microchannels in the honeycomb equals $|OS| = 0.184\,\text{mm}$ and the length of the longest segment in cross section of the microchannels in the honeycomb equals $|OL| = 0.834\,\text{mm}$, do not suggest any strong correlation with the mole fraction. Nevertheless, these dimensions are connected with the velocity field and are presented in Figure 7. The differences between the selected cross sections, specifically $L = 0\,\text{mm}$; $2\,\text{mm}$; $10\,\text{mm}$; $25\,\text{mm}$ occur due to the thermocatalytic surface decomposition which starts at the inlet to the honeycomb and also because of the diffusion effects and volumetric reactions. Hence, with a further increase in the decomposition process, the mixture accelerates due to the increasing mixture mole number. The progress of the velocity field is rapid through $L = 0\,\text{mm}$; and consecutive cross sections $L = 2$; 4; 6; $8\,\text{mm}$; up to the distance of about $L = 10\,\text{mm}$ where the decomposition is complete. Another process, predominantly mixing due to the eddy turbulence, can be observed at the outlet of the microchannels in the honeycomb, $L = 25\,\text{mm}$.

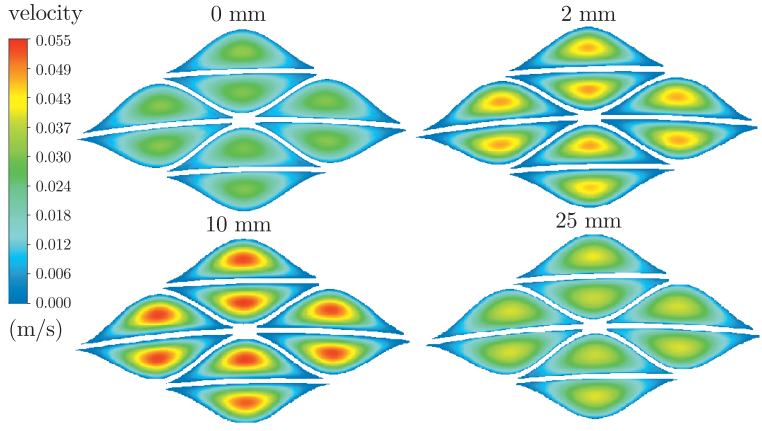

Figure 7. Velocity field at eight single microchannels in cross section presented in Figure 3, namely: $L = 0\,\text{mm}$; $2\,\text{mm}$; $10\,\text{mm}$; $25\,\text{mm}$

5. Conclusions

This paper is concerned with of the modeling of hydrogen production by methanol decomposition in a thermocatalytic reactor based on the intermetallic phase of Ni_3Al. The numerical simulation was performed via the CFD procedure with extensions including the increased chemical reactions rate at the interphase

between the fluid and the solid. The presented analysis should be considered as having demonstrated a promising concept of chemical processing possibilities. The results obtained through numerical calculations were calibrated and compared with the experimental data to receive satisfactory agreement, nevertheless, a more sophisticated approach will be considered which includes the effects of deposit growth on the reaction conditions and the temperature field at the wall. The influence of the temperature will be added as soon as new experimental data is available which will allow the code to be enhanced accordingly. Carbon formation could be modeled by introducing the Lagrange formulation. Therefore, the boundary conditions including fluid-solid interactions should be extended with respect to the carbon nanotube formation.

The original methodology of the 3D numerical analysis for the thermocatalytic micro-reactor used in the decomposition of methanol is presented in this paper. The data extrapolated via the implemented numerical model made it possible to assess the minimal length of the microreactor channels, which provide a full conversion of methanol at the system outlet.

Acknowledgements

The results of the work were obtained in studies co-financed by the National Research and Development Centre under Project PBS3 ID 246201 entitled: "The development of innovative technology, thin foils of alloys based on intermetallic phase Ni_3Al with high activity thermocatalytic in the field of purification of air from harmful substances or controlled decomposition of hydrocarbons."

References

[1] Jóźwik P, Grabowski R and Bojar Z 2010 *Mater. Sci. Forum* **636–637** 895
[2] Olafsen A, Daniel C, Schuurman Y, Raberg L B, Olsbye U and Mirodatos C 2006 *Catal. Today* **115** 179
[3] Jóźwik P, Polkowski W and Bojar Z 2015 *Materials* **8** 2537
[4] Moussa S O and El-Shall M S 2007 *J. Alloys Compd.* **440** 178
[5] Xu Y, Ma Y, Sakurai J, Teraoka Y, Yoshigoe A, Demura M and Hirano T 2014 *Appl. Surf. Sci.* **315** 475
[6] Badur J 2003 *Numerical modelling of sustainable combustion in gas turbines*, IFFM Publlishers
[7] Kuo K K and Acharya R 2012 *Applications of turbulent and multiphase combustion*, John Wiley & Sons
[8] Williams F A 1965 *Combustion theory*, Addison Wesley
[9] Chen G-B, Chen C-P, Wu C-Y and Chao Y-C 2007 *Appl. Catal. A* **332** 89
[10] Jóźwik P, Badur J and Karcz M 2011 *Chemical and Process Engineering* **32** (3) 215
[11] Aoki N, Yube K and Mae K 2007 *Chem. Eng. J.* **133** 105
[12] Duran J E, Mohseni M and Taghipour F 2010 *Chem. Eng. Sci.* **65** 1201
[13] Mitani H, Xu Y, Hirano T, Demura M and Tamura R 2017 *Catalysis Today* **281** 669
[14] Michalska-Domańska M, Bystrzycki J, Jankiewicz B and Bojar Z 2017 *Comptes Rendus Chimie* **20** 156
[15] Badur J, Ziółkowski P J and Ziółkowski P 2015 *Microfluid Nanofluid* **19** 191
[16] Badur J, Ziółkowski P, Sławiński D and Kornet S 2015 *Energy* **92** 142
[17] Modliński N 2014 *Chemical and Process Engineering* **35** 361
[18] Modliński N, Madejski P, Janda T, Szczepanek K and Kordylewski W 2015 *Energy* **92** 77

[19] Weber R, Schaffel-Mancini N, Mancini M and Kupka T 2013 *Fuel* **108** 586
[20] Ziółkowski P, Stajnke M and Jóźwik P 2017 *Transactions IFFM* **138** 33
[21] Flaszyński P, Doerffer P, Szwaba R, Kaczyński P and Piotrowicz M 2015 *Journal of Thermal Science* **24** (6) 510
[22] Badur J, Ziółkowski P, Zakrzewski W, Sławiński D, Kornet S, Kowalczyk T, Hernet J, Piotrowski R, Felicjancik J and Ziółkowski P J 2014 *J. Phys.: Conf. Ser.* **530**
[23] Pianko-Oprych P, Kasilova E and Jaworski Z 2014 *Chemical and Process Engineering* **35** 293
[24] Badur J, Karcz M, Lemański M and Nastałek L 2011 *CMES: Computer Modeling in Engineering & Sciences* **73** 299
[25] Ziółkowski P and Badur J 2018 *International Journal of Numerical Methods for Heat and Fluid Flow* **28** (1) 64
[26] Lewandowski T, Ochrymiuk T and Czerwińska J 2011 *ASME Journal of Heat Transfer* **133** 22401